Accepted Manuscript

Title: History of mass measurements in time-of-flight mass analyzers

Author: Hermann Wollnik
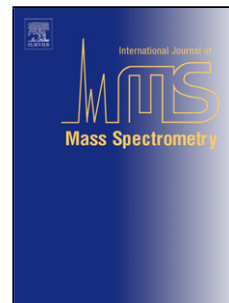
Please cite this article as: H. Wollnik, History of mass measurements in time-of-flight mass analyzers, *International Journal of Mass Spectrometry* (2013), http://dx.doi.org/10.1016/j.ijms.2013.04.023

History of mass measurements in time-of-flight mass analyzers

Hermann Wollnik

2. Physikalisches Institut, Universität Giessen in Giessen, Germany and
Chemistry Department, New Mexico State University in Las Cruces, NM, USA

Abstract

Time-of-flight mass analyzers have been developed since the 1950s, but there was a 30 year period during which new developments were slow. However, in the 1980s new ideas were proposed for the mass analysis of high energy ions, allowing an overview of the masses of most existing nuclei, and for low energy ions a fast and accurate identification of large molecules became possible. Since the 1990s especially multi-pass energy-isochronous time-of-flight mass analyzers have been developed for high as well as for low energy ions.

1. Introduction

The masses of atomic and of molecular ions have been measured with ever increasing accuracies since the early 1900s in order to determine the isotopic composition and nuclear binding of stable and of radioactive atomic nuclei and in order to identify molecules by their weights as desired by medical, chemical, and geological research. Both these measurements require mass analyzers that have high mass resolving powers $R_M = M/\Delta M$ but also high ion transmissions. For the early on available laterally dispersive static sector-field mass analyzers this ion transmission is proportional to the lateral phase space area σ_X of an ion beam, i.e. the product of its lateral width and the maximal lateral angles of inclination of ion trajectories in the ion beam. On the other hand the mass resolving power of such mass analyzers is proportional to $1/\sigma_X$ since the product $R_M \sigma_X$ is a constant for a given system [1], stating that the mass resolving power R_M can only be increased if the ion transmission is reduced.

Such a limitation does not exist for a longitudinally dispersive time-of-flight mass analyzers described in 1949, in which pulsed ion beams would be injected into static electromagnetic fields [2] and the mass characterizing ion flight times through the system be measured. In such time-of-flight mass analyzers the ion transmission is also proportional to the lateral phase space area σ_X while the mass resolving power depends on the longitudinal phase-space distribution of the ions in a packet, i.e. the product of the length of an ion packet and the maximal differences of velocities of the contained ions, showing that the mass resolving power and the ion transmission could both be optimized independently, so that major improvements in precision and accuracy of mass measurements became feasible. However, new time-of-flight mass analyzers had to be designed, constructed and built in which short ion packets were not elongated during their flight through the system. Note here also that in order to form short ion pulses

and to quickly record ion arrival times these time-of-flight mass analyzers required fast electronic circuitries, techniques which only started to become available in the 1950s and 1960s.

Demands on the performance of time-of-flight mass analyzers

A prerequisite to design high performance time-of-flight mass analyzers was to extend the ion-optical description of ion transfer between entrance and exit of a system for which ion flight times were important. Such a transfer is best described [3, 4] by a transfer matrix which reads to first order for ions of equal masses:

$$\begin{pmatrix} X_{i+1} \\ A_{i+1} \\ \delta K \\ \delta T_{i+1} \end{pmatrix} = \begin{pmatrix} (X|X) & (X|A) & (X|\delta K) & 0 \\ (A|X) & (A|A) & (A|\delta K) & 0 \\ 0 & 0 & 1 & 0 \\ (\delta T|X) & (\delta T|A) & (\delta T|\delta K) & 1 \end{pmatrix} \begin{pmatrix} X_i \\ A_i \\ \delta K \\ \delta T_i \end{pmatrix} \tag{1}$$

where X and A describe the position and angle of inclination of the trajectory of an arbitrary ion at the entrance to the time-of-flight mass analyzer relative to a system axis along which a reference ion can move, while $\delta K = (K/K_0 - 1)$ and $\delta T = (T/T_0 - 1)$ are relative energy and time deviations, and the indices i and $i + 1$ denote these quantities at the entrance and at the exit of the system under consideration. Furthermore K_0 and K describe the energies of a reference ion and of an arbitrary ion, respectively, while T_0 and T describe the times when a reference ion and when an arbitrary ion enters or leaves the time-of-flight mass analyzer, respectively. The matrix elements in Eq.(1) were determined by algebraic ray tracing calculations for slow and for relativistically fast ions [4,5,6] so that the design of new high performance systems could start in the early 1980s for low- and for high-energy ions.

For most applications of time-of-flight mass analyzers the ions to be investigated have large energy spreads δK and originate from low intensity sources. Thus it was most important that the electric or magnetic fields in the time-of-flight mass analyzer were shaped

1. so that ions of different energies pass through the system in the same time and thus are "energy-isochronous" requiring that in Eq.(1)

$$(\delta T|\delta K) = 0 \tag{2a}$$

2. and that ions that have passed through the system entrance are guided by electric and/or magnetic fields so that those that have passed through the system entrance also pass through the system exit independent of the initial inclinations of their trajectories and of their energies, i.e. the system is "stigmatic and achromatic focusing". For the energy-isochronous time-of-flight mass analyzer one thus must postulate [4] that each of them fulfills Eq. (2a) as well as

$$(X|A) = (A|X) = (A|\delta K) = 0 \tag{2b}$$

2

so that the ion trajectories are mirror symmetric for the system.

These design goals were achieved in the early 1980s when the systems were designed from mirror symmetric or two- and four-fold arranged magnetic sector field sub-systems [7, 8]. This design already pointed the way for all later to come high performance time-of-flight mass analyzers used for the mass analysis of high- and low-energy ions. In all these designs, however, some of the high-order coefficients of flight time aberrations stayed finite and here especially those proportional to some higher power of the energy spread δK of the ions under investigation, which suggests that this energy spread of should always be kept as small as possible.

3. Time-of-flight mass analyzers for high energy ions

The first high performance energy-isochronous time-of-flight mass analyzers were designed and built to determine masses of energetic short-lived nuclei. For such ions their flight times through a mass analyzer can be determined very accurately by using, one start detector placed at the entrance and one stop detector placed at the exit of the time-of-flight mass analyzer. On way to build such detectors [10] is to use a thin converter foil from the surface of which secondary electrons are released when energetic ions pass through the foil, wherein this release of secondary electrons is increased if this surface is coated with CsI. These electrons are then guided by electromagnetic fields of the detector to a fast channel plate amplifier, whose signal accurately marks the ion passage time. In an arrangement of start- and stop detectors 100% of the existing ions are recorded as long as they produce signals in both thin foil detectors, while the energy loss of a few keV during passage through the converter foil is negligible for high energy ions.

3.1 Energy-isochronous time-of-flight mass analyzers for high energy ions

A first energy-isochronous time-of-flight mass analyzer for energetic ions was built [8,10] in Los Alamos, NM in the USA in the early 1980s named time-of-flight isochromat (TOFI). This instrument was built as a symmetric arrangement of 4 identical subsystems since this provided very good first and second order properties [11]. Each of these subsystems comprised one sector magnet with inclined boundaries (see Fig. 1), wherein each subsystem was designed so that it fulfilled Eqs. (2) and where additionally the transversal and longitudinal aberrations of higher-order stayed within limits [12]. Thus substantially all ions that had passed through a small thin-foil start detector at the entrance of TOFI were guided to a small thin-foil stop detector of equal area placed at the exit of TOFI. A more technical limitation for TOFI was that its overall flight path was 14m resulting in overall flight times of only ≤1μs for the ions of interest. In order to achieve a good flight time resolving power and thus a good mass resolving power, the time signals of the start- and stop-detectors [9] had to be very, very precise. These short flight times on the other hand made it possible to perform mass measurements in times that are short when compared to the life time of most nuclei and even isomeric states of them.

Also in the early 1980s a not energy-isochronous time-of-flight mass analyzer SPEG was built [13] in Caen, France, the ion flight path in which was 82m, i.e. about 6 times longer than the flight path in TOFI and so yielded better precisions for the flight time measurement. However, in this system the ion energy had to be determined in a magnetic sector field spectrograph, which was achieved with errors of only ≈100ppm. Knowing the ion energy so precisely, the ion flight times could be energy corrected and the ion masses be determined with good precision.
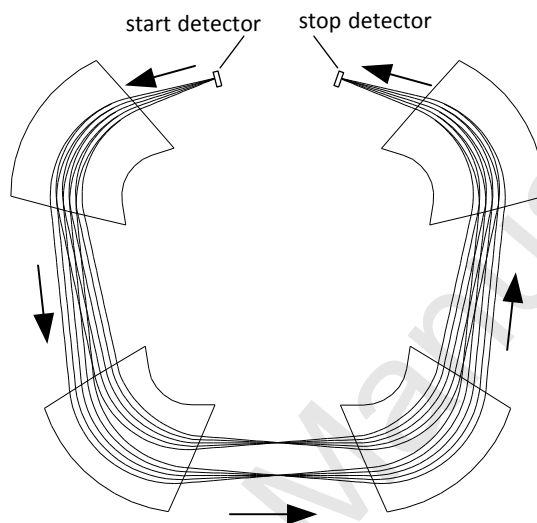

Fig. 1 Sketch of ion trajectories in TOFI the first energy-isochronous time-of-flight mass analyzer for high energy ions. This system contained 4 sector magnets of deflection radii of 1.1m and deflection angles of 81° with entrance and exit angles $\epsilon = 15°$ forming an overall flight path of 14m in length.

With both TOFI and SPEG good mass measurements of short lived nuclei could be performed [14, 15]. However, even more precise measurements were desired. For an energy-isochronous time-of-flight mass analyzer this goal was pursuit by attempting to increase the length of the overall flight path, which was planned to be achieved by building mass analyzers in which the ion deflection was 360°, so that the ions could move repeatedly through the resulting ring. Such a solution, however, required to find a good ion-optical design that turns such a ring into a good time-of-flight mass analyzer that is energy-isochronous per lap as well as achromatic and stigmatic focusing and whose flight time aberrations were small.

3.2 Multi-pass time-of-flight mass analyzers for high energy ions

When considering how to arrange a large ring of magnets so that they act as a time-of-flight mass analyzer, the idea arose to not build such a system but to search for an existing accelerator storage ring and see whether it could be modified so that mass measurements can be performed for the circulating ions. Especially interesting was to find out whether the condition of energy-isochronicity, i.e. Eq. (2a) could be fulfilled for such a storage ring by simply varying the strengths of its quadrupoles which would

4

not require to change the structure of the ring. After lengthy calculations such a solution seemed feasible for the "experimental storage ring" (ESR) of the heavy ion research center GSI in Germany, as was proposed already at the occasion of its inauguration in 1985. At the end [16, 17] there were even two methods (see Fig. 2) both of which could precisely determine ion flight times and thus ion masses by using the ESR as a multi-pass time-of-flight mass analyzer.

1. In the first case [16] ion beams are injected into the ESR with energy spreads δK of ≈1%. In this case the strengths of the quadrupoles of the ESR were changed so that its optical tune was changed, which reduced the maximal ion intensity to about half, but which allowed to fulfill the energy-isochronous condition of Eq. (2a) for every lap. Operating the ESR in this way was named operating it as an "IMS" or isochron mass spectrograph.

2. In the second case [17] ion beams are injected into the ESR as well as a beam of electrons that have the same velocity as the average velocity of the ions. This caused interactions between the ions and the electrons, which reduced the ion velocity spread of the ions to approximately that of the electrons. At the end this process reduced the ion energy spread δK to about 1ppm so that the ion flight time per lap depended substantially only on the ion mass. In this case the frequency of ion passes is recorded by induced image currents in a capacity probe, also called a Schottky noise-pickup. Operating the ESR in this way was named operating it as a "SMS" or Schottky mass spectrograph.

Both techniques are best understood [18] when one describes the mass resolution $\Delta m/m$ as function of the frequency resolution $\Delta f/f$ and the relative spread of the ion velocity $\Delta v/v$ to first order as:

$$\left| \frac{\Delta m}{m} \right| = \gamma_t^2 \left| \frac{\Delta f}{f} \right| + (\gamma_t^2 - \gamma^2) \left| \frac{\Delta v}{v} \right| \tag{3}$$

Here γ is the relativistic Lorentz-factor for the ion motion and γ_t characterizes this factor for that case in which the condition of energy-isochronicity [see Eq. (2a)] is fulfilled. The IMS case thus is characterized by $\gamma = \gamma_t$ and the SMS case by $\Delta v = 0$.
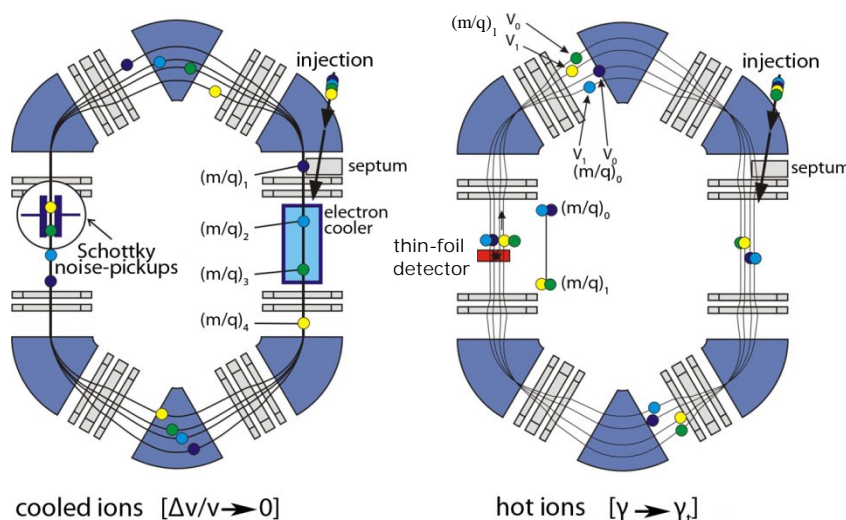
5

Fig.2 Shown are two ways how the ESR of the GSI of ≈100m circumference can be used as a multi-pass time-of-flight mass analyzer in order to precisely determine the masses of circulating ions. On the right is shown how the ions move, when the storage ring is operated as an IMS, i.e. an energy-isochronous time-of-flight mass spectrograph, in which the ions pass through a thin foil detector in every lap. On the left is shown how cooled ions move, when the storage ring is operated as a SMS, i.e. a Schottky time-of-flight mass spectrograph, in which case the frequencies of ion passes are recorded by image currents in a Schottky noise-pickup.

Mass measurements were performed with both techniques achieving [19] mass resolving powers of 100,000 or more and mass precisions of ≥100keV in both cases. Very importantly both methods allowed to record in one experiment the flight times of ions of a range of masses of several percent as in classical laterally dispersive mass spectrographs. In the time up to the present the masses of a large portion of all known nuclei have been determined [20] by these two methods at the ESR or at the new facility in Lanzhou, China [21].

3.2.1 Using the ESR storage ring as an SMS with cooled ions

To operate the ESR with cooled ion beams had been planned from the beginning of its construction and in 1992 it was proven [18] that energetic ions could be cooled to energy spreads of ≈1ppm which allowed precise mass measurements [18]. In the Mid 1990s already [22, 23] it was possible to operate the ESR as a multi-pass time-of-flight SMS and determine precise masses of cooled stable and short-lived nuclei, when the signals of the Schottky noise-pickup in the ESR were Fourier-analyzed. This technique provided highly resolved mass spectra (see Fig.3) of stable nuclei as well as of those with life times in the range of seconds or longer with mass resolving powers of 350,000. In the first extended mass measurements in 1997 already the masses of more than 100 nuclei could be determined, whose masses were not known before.
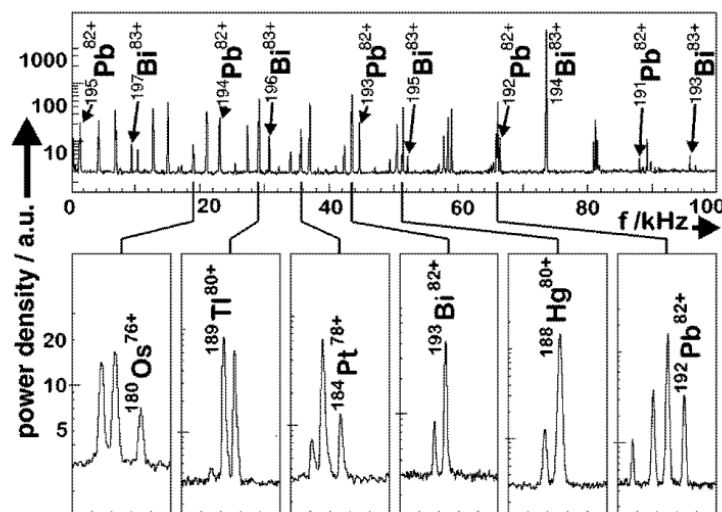
6

Fig.3   Shown is a wide range highly resolved mass spectrum recorded of cooled ions that circulate in the ESR and are recorded by image currents induced in a low capacity probe, a so-called Schottky noise-pickup. Note that the highly resolved sections in the lower part of this figure are ≈1kHz wide showing that high mass resolving powers are achieved over a wide mass range.

In these first experiments also several of the investigated nuclei were those at the end points of α-decay chains, in which cases also the masses of all members of these chains became known including those close to the proton drip line. In later experiments [24] in 2005 mass resolving powers of 500,000 were obtained and mass precisions of ≈100keV.

To cool ions of interest requires always relatively long cooling times, which also in good cases are a few seconds or more. Very short lived nuclei thus may have partially decayed already during this time. For this reason the SMS method can only be used for ions of reasonably long life times though its mass resolving power and mass range are superb.

3.2.2 Using the ESR storage ring as an IMS with hot ions

To operate the ESR as a multi-pass energy-isochronous time-of-flight mass analyzer [16], i.e. an IMS, was tested experimentally [25, 26] in 2000. To determine the ion flight time in such a system a dedicated thin-foil detector [27] was placed into the ESR in the Mid 1990s so that the passes of individual ions
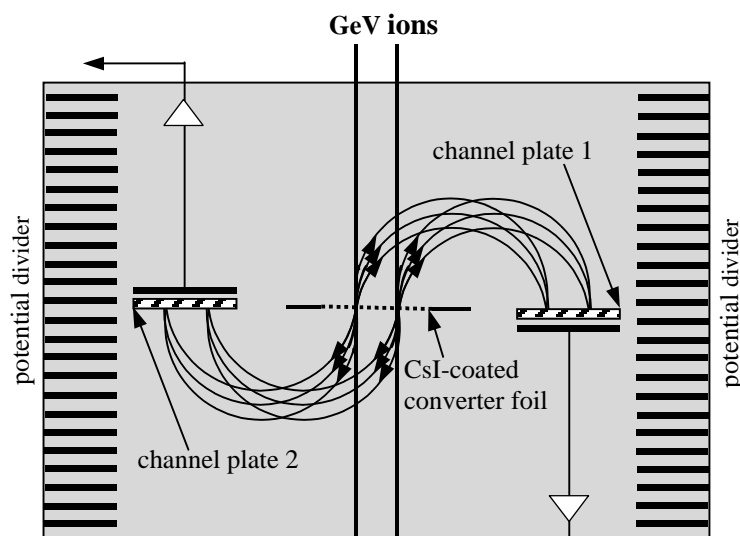
Fig. 4 Troetscher's thin foil detector developed to record the passing of ions for every lap in the
ESR. Please note that the secondary ions released from the front and the back of the
converter foil are all guided to channel plate detectors.

could be monitored for every lap of the circulating ions. This detector is similar to the one [10] used at
TOFI in the early 1980s though it made use of secondary electrons released from both sides of the
covered converter foil that are deflected in a large low field magnet as is illustrated in Fig. 4. This was of
advantage, since the release of secondary electrons has only a finite probability. This result was even
improved by covering the converter foil on both sides with CsI that has a low work function.

A real record of the signals of this detector is shown in Fig.5 when three ions were circling in the ESR. In
Most cases the passing of ions could be recorded over several 100 or even several 1000 laps until
eventually the ions were lost because of small angle scatterings in the converter foil.
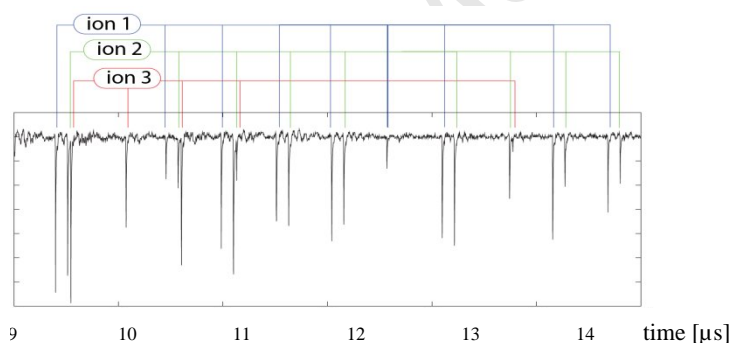

Fig. 5 Shown are the signals obtained from a thin foil ion detector placed into the ESR to record ions after each
lap of the in the ESR circulating ions during the first experiments in 1997. Note that in this figure the
signals of secondary electrons were recorded, when an ion passed through the converter foil. Note also
that the signals had different amplitudes and that at some cases no signal was seen, though certainly an
ion had passed through the converter foil. Both effects resulted from the finite probability of the release
and detection of secondary electrons.

For the operation of the ESR as an IMS it was essential that the ions' energy spread δK was limited by
passing the ions of interest first through the "fragment separator" FRS [28] of the GSI that selected the
ions according to their momentum/charge. This limitation of δK was advantageous for the mass
measurements, because so the higher-order flight time aberrations of the ESR were reduced. During the
first IMS operation in 2000 already mass resolving powers of ≈100,000 were achieved and mass
precisions of 100 to 500 keV. Eight years later the achieved mass resolving power had been increased
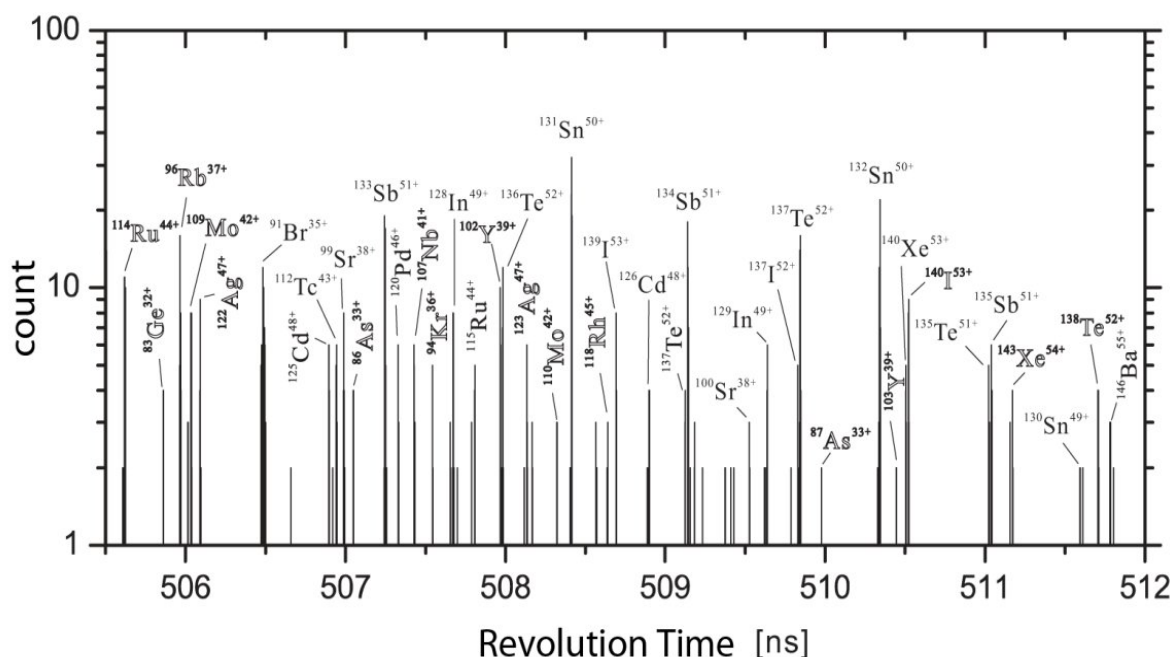
8

Fig. 6 A good IMS mass spectrum is shown of ref. [30] illustrating that the masses of a multitude of
known (bold face letters) and previously unknown (outlined letters) nuclei can be determined
quasi simultaneously.

[29] to ≈200,000 mainly by defining the momentum/charge of every ion individually [30] by the FRS with
a precision of a few 100ppm. At the end this allowed mass precisions of ≈100keV for most registered
ions over mass ranges of several percent.

Since the ion flight time for one lap is around 0.5µs in the ESR, the overall ion flight time in the ESR for
an IMS operation is mostly a few 100µs. This time is long enough to determine the ion flight times
accurately and so achieve good mass resolving powers, but it is also short enough that the masses of
most short lived nuclei can be determined down to the microsecond range in case of isomers.

4. Time-of-flight mass analyzers for low energy ions

Time-of-flight mass analyzers for low energy ions are almost exclusively built from electric fields and are
mainly used to identify molecules by determining their masses. This task requires efficient ion sources
for organic molecules which unfortunately all produce ions with a sizeable energy spread δK. Thus, it is
very desirable that a time-of-flight mass analyzer used for their mass analysis is energy-isochronous, i.e.
built so that Eq. (2a) is fulfilled. The first such time-of-flight mass analyzer [31] existed already in 1955.
New improved, now all energy-isochronous time-of-flight mass analyzers, appeared only in the 1980s.

4.1 Formation and recording of short ion pulses

To determine the flight time of low energy ions through a time-of-flight mass analyzer it is necessary to
form short ion pulses. One way, that was started in the late 1980s, is to use a "matrix assisted laser

9

desorption ion source" (MALDI) [32]. In this ion source an intense pulsed laser beam is directed onto a liquid, in which analyte molecules are dissolved. This energy impact forms small droplets of this liquid and at the end produces an intense short pulse of ionized analyte molecules, which then are accelerated in static electric fields to a few keV.

A more general way to form short pulses of ions is to use existing ion sources that produce a continuous beam of ions and establish during short periods an electric field E_a that accelerates the ions of this beam orthogonal to its beam axis. In such an arrangement the ions that started closer to the grid that is at an ion attracting potential, will be accelerated to lower energies than those that started further away from it. As a result of this the different ions will catch up with each other a short distance downstream from this grid and form there a short packet of ions, whose energy spread δK is large, however. For a mass analysis of these ions consequently an energy-isochronous time-of-flight mass analyzer is very desirable. This technique had been used already in the first fully functioning time-of-flight mass analyzer [31] introduced in 1955, wherein also an attempt was made to improve the situation by post accelerating these ions from the catch-up point and by doing this with a short delay so that ions of higher energy had moved already a little further in the acceleration direction and thus were accelerated less than ions of lower energy.

In reality the ions in the initial ion beam are inclined relative to each other and thus have always a small initial velocity $\pm v_0$ perpendicular to the axis of the ion beam, i.e. in the direction of the pulsed ion acceleration field E_a. In this field the ion velocity $+v_0$ is reduced to zero in a time τ_v. The accelerated ions in this pulse thus have a minimal duration of $2\tau_v$, the so-called turn-around time [33, 34], which is usually a few ns long and decreases if the magnitude of E_a is increased. This is the reason that all high performance time-of-flight mass analyzers use quite high values of the pulsed field E_a even if this technologically is not simple.

During the late 1980s several steps were taken to reduce this velocity and thus the turn-around time. There was:

1. The orthogonal extraction technique [34, 35, 36], in which prior to the acceleration of ions perpendicular to the beam axis by an electric field, the ion beam was formed by static quadrupoles so that it was widened (see Fig.7) in the direction of E_a and compressed in the perpendicular direction. This widening of the ion beam in the direction of E_a reduced the inclination of ion trajectories relative to each other and thus the ion velocities $\pm v_0$ in the direction of E_a. After acceleration only these very small velocities $\pm v_0$ caused the turn-around time $2\tau_v$.

2. The method of accumulation, storing and cooling of ions in a gas-filled potential depression region formed by three grids of which the potential of the middle grid was lower than the potentials of the other two [33, 34, 37]. In such a potential depression region the ions swing forth and back between the two outer grids so that because of collisions with residual gas

10

atoms or molecules the ion energies are reduced the those of the atoms of molecules at room temperature and thus to ≤0.2eV. Only after the ions were cooled, they were extracted into the time-of-flight mass analyzer by an electric dipole field E_a suddenly superimposed over the stored ion cloud.

3. This gas-filled potential depression region was also replaced by a gas-filled quadrupole ion trap [38] in which the ions could also be cooled to ≤0.2eV. This method was especially effective when the quadrupole field were formed in a quadrupole field formed by printed circuit electrodes. The reason is that this field can be changed from the RF-quadrupole field to a good static dipole field [39] at the time of ion extraction in which case the ions are extracted perpendicularly to the quadrupole axis as a low phase space ion beam.

4. Even better ion cooling results were achieved by an RF-only quadrupole [40, 41, 42] which in turn allowed improved mass resolving powers of the time-of-flight mass analyzer. Besides improving the molecule identification by a more precise mass measurement, this RF-only method allowed to simultaneously characterize molecules by their fragmentation properties [43] as caused by collisions with residual gas atoms or molecules. In this particular arrangement not only the RF-voltage of several MHz was applied to the quadrupole electrodes but also a voltage of several 10KHz which caused the ions to rotate around the quadrupole axis with a frequency dependent speed that controlled the energy transfer in the mentioned collisions.

Being able to start ions in a very short packet it was still necessary to precisely determine at the exit of a time-of-flight mass analyzer the arrival times of ion subgroups of this packet that had the same mass/charge ratio. In the 1950s and 1960s open electron multipliers were used for this purpose. Real improvements were achieved, however, only in the 1970s and 1980s, when channel plate amplifiers became widely available [44]. Today the ion detectors of most high performing time-of-flight mass analyzers use a technique [45] similar to the thin-foil detectors developed [10] for high energy particles in which case. The main difference is that low energy ions do not pass through the converter foil but stop on its front side.

At the end a full mass spectrum could be obtained of the ions contained in each ion packet by recording at the exit of a time-of-flight mass analyzer the arrival times of groups of ions of equal mass/charge ratios with the analysis time of the ions in one packet being a few 100μs. Thus, such a time-of-flight mass analyzer could be well used as a fast "mass spectrograph" to record ions formed from the effluent of a chromatograph [46], in which analyte ions appear in pulses of ≥0.1s in gas chromatographs (GC) and of ≥1s in liquid chromatographs (LC) at times that are characteristic for chemically different molecules. This combination of a chromatograph and a time-of-flight mass analyzer was started in 1994, providing a new powerful two-dimensional characterization of molecules in which mass spectra were recorded for molecules that were selected already for their chromatographic properties.

11

4.2 time-of-flight mass analyzers that use flat repelling fields

Improvements of the time-of-flight mass analyzers [31] that existed in 1955 started only 20 years later, when ions were injected into an electric retarding field [47] that was strong enough to act as an ion mirror and at that would send more energetic ions on a detour relative to ions of lower energy so that the system became energy-isochronous. A time-of-flight mass analyzer that employs such an ion mirror is shown in Fig.7 together with a substantially orthogonal ion injection [34, 36] into a simple to construct flat homogeneous electric mirror field $E_{Z0} = const$. This electric field is established by a potential difference between a flat back plane and a thereto parallel flat grid both being perpendicular to a Z-axis . In Fig.7 also trajectories are shown of two ions of equal mass/charge ratios $(M/Q)_0$ and different energy to charge ratios $(K/Q)_0(1 + \delta K)$ where one of these ions is a reference ion for which δK vanishes.
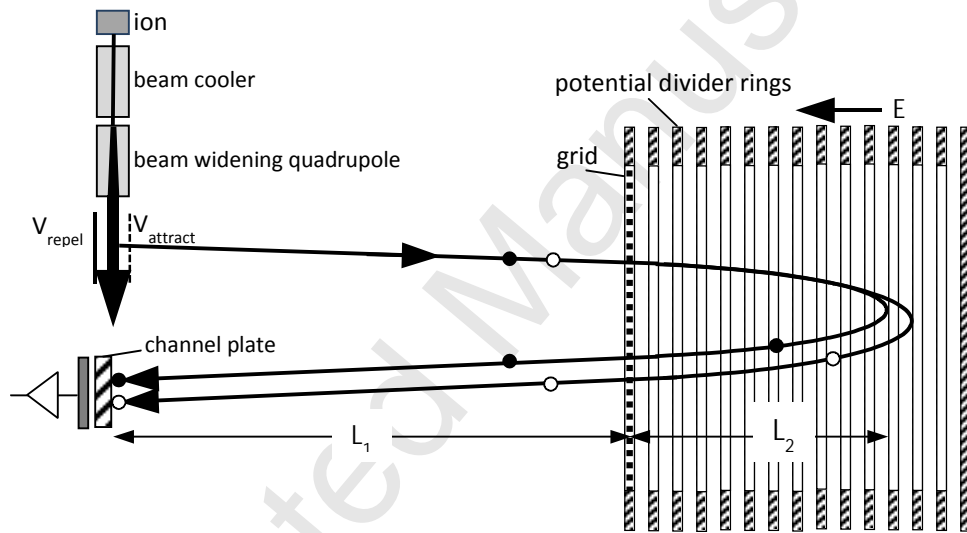

Fig.7. An energy-isochronous time-of-flight mass analyzer formed by a homogeneous electrostatic mirror field E_{Z0} combined with two field-free regions of lengths L_1 is shown together with trajectories of two ions of energy/charge ratios $(K/Q)_0(1 + \delta K)$ wherein the bold circles characterize an ion for which $\delta K = 0$ while the outlined circles characterize an ion of higher energy/charge. Shown is also an orthogonal ion acceleration arrangement in which slow moving ions pass through a cooler quadrupole and a static beam-widening lens arrangement through which the ions pass before they are accelerated into the ion mirror by pulsed potentials V_{repell} and $V_{attract}$.

The Z-components of the velocities of these ions are in the field free region $v_z = v_{z0}\sqrt{(1 + \delta K)}$ which in the electric mirror field first reduce and then increase again after reaching their turn around point at their maximal penetration depths $L_2(1 + \delta K) = (Mv_{z0}^2/2QE_{Z0})(1 + \delta K)$ with an average velocity of $v_z/2$. Calculating the overall flight time for these ions and expanding it in a power series in δK one finds:

$$T_0(1 + \delta T) = [T_0[1 + (\delta T|\delta K)\delta K + (\delta T|\delta K^2)\delta K^2 + \cdots] \qquad (5)$$

12

with $T_0 = 2(2L_2+L_1)/v_{z0}$ and $(\delta T|\delta K) = (2L_2 - L_1)/(4L_2 + 2L_1)$ and a so far undetermined coefficient $(\delta T|\delta K^2)$ of a second order flight time aberration. Choosing $L_1 = 2L_2$ the time-of-flight mass analyzer is to first order energy-isochronous, since $(\delta T|\delta K)$ vanishes and the overall flight time is $4L_1/v_{z0}$ for ions of all energies.

For all these considerations it was quietly assumed that the grid shown in Fig.8 is so fine that it approximates a dipole sheet. In reality, however, the meshes of this grid are finitely large and the electric field E_{Z0} can reach through them, so that a multitude of parallelly arranged small electric lenses is formed, each of which has a focal length $F = 2(K/Q)_0/E_{Z0}$ for reference ions. Ion trajectories that were initially parallel thus become slightly inclined (see Fig.8) to each other and cause differences in the lengths of their flight paths that limit the achievable time resolving power. Herein these differences reduce with the magnitude of F and with the inverse of the size of the meshes of the grid.
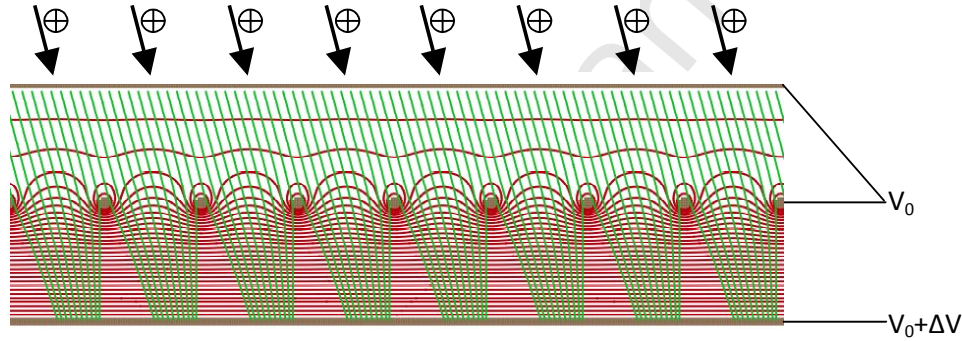

Fig.8. Shown are equipotential surfaces close to the grid shown in Fig. 7 that separates the field-free region from the region in which a field E_z exists. Since this field E_z penetrates slightly through the meshes of this grid, the equipotential surfaces are not planes but bumpy surfaces that act on the ions passing through the grid as a multitude of small lenses.

As a consequence of this, it seemed advantageous to build time-of-flight mass analyzers that use electrostatic mirror fields in which the grid, shown in Fig. 7, was removed. This resulted in an extended fringing field in the now grid-free ion mirror, which complicated the theoretical description of the time-of-flight mass analyzer in a major way, but which simplified its technical design noticeably. At the same time this improved the overall ion transmission to ≈100%, since losses on grid wires did not exist anymore. In this case the homogeneous reflector field E_{Z0} was replaced [34,47] by an inhomogeneous one, in which the Z-dependence of the electric field was controlled by the potentials applied to the potential divider electrodes shown in Fig.7 and the description of the ion motion had to be obtained from direct ray tracing calculations.

The most accurate method to obtain an optimized inhomogeneous field distribution $E_z(Z)$ seems to have been shown [49] in the late 1980s. There the ions of the lowest energy/charge ratio $(K/Q)_1$ produced in the ion source were traced numerically up to their turn around point Z_1 in the electric mirror field. In a

13

small region $Z \geq Z_1$ then the field $E_z(Z)$ was postulated to be changed in such a manner that ions of slightly higher energy/charge ratios $(K/Q)_2$ and thus higher velocities, that reached the position Z_1 earlier, but penetrated deeper into the electric mirror field, arrived at their turn around point at the same time as the ions of energy/charge ratio $(K/Q)_1$ reached theirs. Performing this procedure for ions of larger and larger energy/charge ratios it is possible to iteratively obtain an inhomogeneous field distribution $E_{z0}(Z)$ for which the aberration terms with δK^2, δK^3, ... in Eq.(5) are all substantially eliminated. As a second step then the potentials of the in Fig. 7 shown potential divider electrodes were changed iteratively to approximate the desired field distribution $E_z(Z)$. The corresponding potential distribution could also be approximated by a second-order polynomial in Z, as was proposed in 2002, and in an even simpler though not as accurate way [50] by the long known method of using two homogeneous electric field regions of different field strengths achieved by adding one grid between the back plane and the grid shown in Fig.7.

So designed energy-isochronous time-of-flight mass analyzers have become most important tools for the identification of molecules in medicine and biology, and are therefore produced every year in increasing numbers by various companies worldwide. Because of their high performance and their robust and relatively simple mechanical design they have substantially replaced the use of laterally dispersive magnetic sector field mass analyzers since the 1990s.

4.21 Energy-isochronous multi-pass time-of-flight mass analyzers that use mirror fields

The mass resolving power of energy-isochronous reflector-field time-of-flight mass analyzers can be several 10,000 and their transmission 100% if the mirror field is grid free. However, the overall flight time in such systems is limited, which causes its mass resolving power to be limited also. An improvement can be achieved by combining two or more grid-free energy-isochronous time-of-flight mass analyzers so that the ion flight path and consequently their ion flight time is increased [48]. This is best achieved for N times four subsystems for each of which Eqs. (2) are fulfilled in order that the ion beam is identical in each of the grid-free subsystems, similar to the design of TOFI of magnetic sector fields shown in Fig. 1.
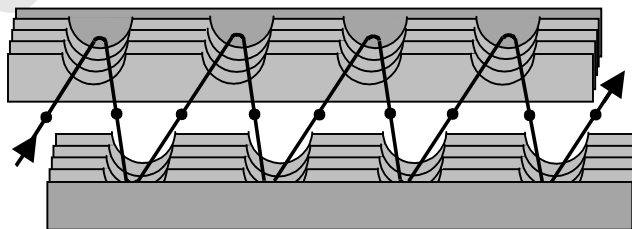

Fig.9. Shown are ion trajectories in the mid-plane of an arrangement of N time-of-flight mass analyzers, wherein the geometry of the overall system is chosen so that it is energy-isochronous. The flight time through these N mass analyzers is N-times longer than that through one of them and this holds also for its mass resolving power.

There are two ways to arrange such mirror-field time-of-flight mass analyzers:

14

1. A first arrangement consisted of several energy-isochronous time-of-flight mass analyzers arranged in series [48, 51]. One such system is shown in Fig.9 illustrating that the overall flight path increases linearly with the number of mass analyzers placed in series. However, this also increases the complexity of the system and thus requires good mechanical and electric precisions and stabilities. Such systems have been built only during the last few years.

2. A second and even more powerful arrangement of energy-isochronous time-of-flight mass analyzers was to arrange two of them so that ions could move through the system repetitively. One such multi-pass time-of-flight mass analyzer is shown in Fig.10 consisting of two energy-isochronous time-of-flight mass analyzers in which the axes of the corresponding ion reflectors coincide [52, 53]. In this system it was postulated that the Eqs. (2) would be fulfilled for every lap and that each mirror field was point-parallel or parallel-point focusing which makes the first order transfer matrix to be a unity matrix for two full laps.

The overall ion flight times as well as the mass resolving powers in such multi-pass systems [48, 52, 53] were dramatically higher than in single pass system, as has been shown in 1990 and 2000. Improvements of 100 or more are certainly feasible for the mass resolving power of such "multi-pass systems". However, while the necessary mechanical tolerances stayed within limits, the demands on the mechanical, electric and temperature stabilities were high.
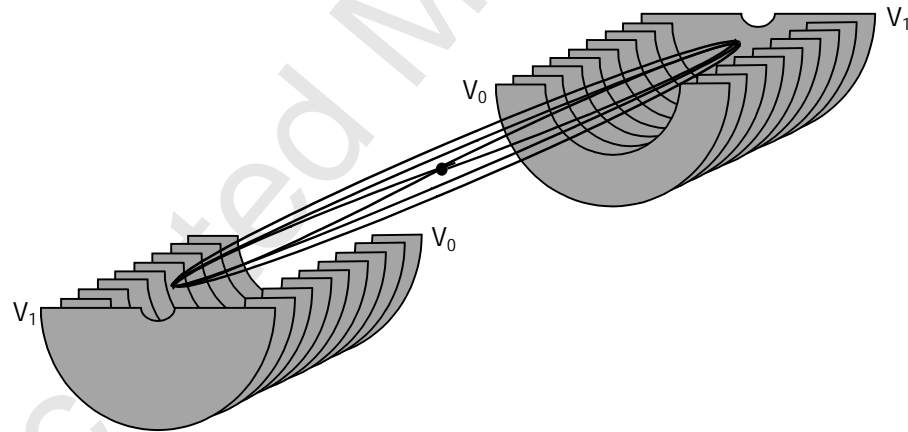

Fig. 10. An arrangement of two mirror type energy-isochronous time-of-flight mass analyzers is shown which together form a multi-pass time-of-flight mass analyzer. The flight time for each lap through this system is energy-achromatic and energy-isochronous. Its overall flight time and thus its mass resolving power depend on the number of laps the ions perform in this multi-pass system.

Also there were two problems when using such multi-pass time-of-flight mass analyzers:

1. As in any accelerator storage ring it is difficult to have ions enter or leave multi-pass systems. In systems that use ion mirrors this problem has been solved by requiring that for the short times of ion entry or exit the maximal mirror potentials of the corresponding ion mirrors are lower than the potential the ions had been accelerated to.

15

2. When recording a full time-of-flight spectrum it will be a superposition of time-of-flight spectra of ions who have performed N, N+1, N+2,…. laps. To untangle these different spectra it is necessary to either allow only ions of a small mass range to enter the system or to determine to which lap number a special mass line belongs from recording several spectra after different laps and observing the variation between them [54].

One such energy-isochronous multi-pass time-of-flight mass analyzer that uses two coaxial ion mirrors has been built as a 0.4m long system of 1.15kg weight so that it can be operated on a space craft [53, 55] which was sent in 2003 to a comet head to be used for in situ material analysis [56]. This small system had achieved mass resolving powers of 16,000 and much higher values [57] in a special laboratory installation.

During the last 10 years several such multi-pass time-of-flight mass analyzers have been built for the precise measurement [58, 59] or for the selection [60, 61] of slowed down short-lived nuclei. These systems achieve routinely mass resolving powers of 100,000 to 200,000 and in special cases even more. Thus, they should be able to rival the precision and accuracy of mass measurements achieved when operating accelerator storage rings as time-of-flight mass spectrographs. However, such systems certainly could also be used advantageously for accurate molecule identifications in medical, biological or chemical investigations.

4.22 Energy-isochronous multi-pass time-of-flight mass analyzers that use electric sector fields

Though multi-pass time-of-flight mass analyzers that use electric reflector fields have achieved high levels of performance, there were also designs that since the 1980s use electric sector fields [62, 63]. Placing four of such sector field time-of-flight mass analyzer in series [62, 64] mass resolving powers ≥100,000 have been achieved [65] in 2011. However, such systems have also been built as multi-pass systems [66] in which ions pass through the same sector fields again and again.
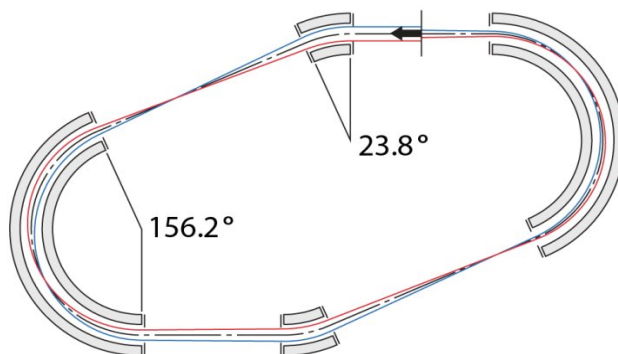

Fig. 11 An arrangement of two double toroidal electric sector fields is shown, who form an energy-isochronous multi-pass time-of-flight mass analyzer. This system can achieve high mass resolving powers if the ions pass often through the ring.

In multi pass time-of-flight mass analyzers mentioned so far individual ions were postulated to move along the same trajectories in different laps [see Eqs. (2)] which postulated for each lap $(\delta t|\delta K) = (X|\delta K) = 0$ so that ions of different energies would arrive at the same time and position after every lap. However, there were also the spatial focusing demands $(X|A) = (A|X) = 0$ for each lap which demanded that the ion trajectories were identical in each lap. As an alternative it is also possible [4] to postulate only that the ions move stably in phase space, which requires only

$$|(X|X) + (A|A)| \leq 2 \tag{4}$$

In this case the individual ions move on different trajectories during different laps. This also avoids that a small construction error at a specific position in the time-of-flight ring causes the same trajectory deviation in each lap. The condition of Eq. (4) had already been considered for mirror type time-of-flight mass analyzers [55]. However, it became essential for sector field systems [66] where, very importantly it gave more freedom to the system designers, so that they could construct a relatively simple ring type instrument sketched in Fig. 11. In order to inject ions into and eject them out of this ring, one of the sector fields must be switched off for a short period and provide from the outside an ion injection and an ion ejection system. Also the problem must be addressed here that in the final recording mass spectra of ions are superimposed that have performed different numbers of laps.

Summary

Altogether one can say that good time-of-flight mass analyzers for low energy ions have been available already since the 1950s, though the great wave of new systems started only in the 1980 driven initially by the demand to provide superior instruments for the mass measurement of short-lived nuclei. This resulted in the building of special instruments and in the transformation of accelerator storage rings into high performance time-of-flight mass analyzers. Following the same principles also new energy-isochronous time-of-flight mass analyzers have been developed since the 1990s for the mass identification of low energy ions of large molecules. These instruments were so successful that today they have substantially replaced the former used laterally dispersive magnetic sector field instruments. Most important was the development of multi-pass systems for high energy ions in slightly remodeled accelerator storage rings, which have become the workhorse for the precise mass measurement of stable and short lived nuclei. Parallel to these developments multi-pass time-of-flight mass analyzers have been built for low energy ions in which ions are multiply reflected between two coaxial electrostatic ion mirrors or in rings of electric sector fields. Such systems can be used for slowed down ions of short-lived nuclei and are looked at as more flexible and more easily modifiable and certainly much cheaper systems than large accelerator storage rings for high energy ions, though the achievable mass resolving powers in both systems are comparable. Their use for the mass identification of low energy ions of large molecules has only started, however.

Acknowledgements

References

1. H. Wollnik, Nucl. Instr. & Meth. 95 (1971) 453

2. A.E. Cameron, D.F. Eggers, Rev. Sci. Instrum., 19 (1948) 605

3. H. Wollnik Nucl. Instr. & Meth. 186 (1981) 441

4. _____ H. Wollnik "Optics of Charged Particles", Acad. Press, Orlando, 1987

5. H. Wollnik, H. Matsuda, Nucl. Instr. & Meth. 189 (1981) 361

6. H. Wollnik, Nucl. Instr. & Meth. A 298 (1990) 156

7. H. Wollnik and T. Matsuo, Int. J. Mass Spectrom. Ion Phys. 37 (1981) 209

8. J.M. Wouters et al.,Nucl. Instr. & Meth. 240 (1985) 77

9. K.H. Kraus, D.J. Vieira, H. Wollnik, J.M. Wouters, Nucl. Instr. & Meth. 269 (1988) 327

10. J.M. Wouters et al., Nucl. Instr. & Meth. B 26 (1987) 286

11. K.L. Brown, IEEE Trans. NS-26 (1979) 3490

12. H. Wollnik, in IFOS-III, ed. A. Benninghoven, Springer Proc. in Phys. 9 (1986) 184

13. H. Savajols, Hyperfine Interactions 132 (2001) 245

14. H. L. Seifert et al., Nucl. Phys. A 349 (1994) 25,
15. G.F. Lima et al., Phys. Rev. C 64 (2002) 44618

16. H. Wollnik, Nucl. Instr. & Meth. B 26 (1987) 267

17. _____ B. Franzke, Nucl. Instr. & Meth. B 24 (1987) 18

18. H. Geissel et al., Phys. Rev. Lett. 68 (1992) 3412

19. _____ H. Geissel, H.Wollnik, Nucl. Phys. A 693 (2001) 19

18

20. K. Blaum et al., J. Phys.: Conf. Ser. 312 (2011) 092001

21. Y. Litvinov et al., Acta Phys. Polonica B 41 (2010) 511

22._____ T. Radon et al. Phys. Rev. Lett. 78 (1997) 4701

23._____ T. Radon et al. Pramana J. Phys. 53 (1999) 600

24._____ Y. Litvinov et al. Nucl. Phys. A 756 (2005) 3

25._____ J. Stadlmann et al. AIP conf. Proc. 512 (2000)
    305

26._____ M. Hausmann et al. Nucl. Instr &Meth A 446
    (2000) 569

27. J. Troetscher, thesis, University Giessen 1993

28. P. Armbruster at al., AIP Conf. Proc. 164 (1988) 839

29. R. Sun et al., Nucl. Phys. A 812 (2008) 1

30. H. Geissel et al., AIP Conf. Proc. 831 (2006) 108

31. W.C. Wiley, Rev. Sci. Instr. 26 (1955) 1150

32. M. Karas, F. Hillenkamp, Anal. Chem. 60 (1988) 2299

33._____ R. Grix et al. Int. J. Mass Spectrom. Ion Proc.
    93 (1989) 323

34. _____H. Wollnik, Int. J. Mass Spectr. Ion Proc. 131
    (1994) 387

35. A.F. Dodonov et al., USSR patent 168134OA1 of 1987
36. A.F. Dodonov, I.V. Chernushevich and V.V. Laiko, ACS Symp. Ser. 549 (1994) 108

37._____ A. Casares, A. Kholomeev, H.Wollnik, Int. J.
    Mass Spectr. 206 (2000) 267

38. C. Weil et al. Rap. Comm. Mass Spectr. 10 (1996) 742

39. P. Schury et al. Eur. Phys. J. A 42 (2009) 343

40. A.V. Tolmachev et al., Nucl. Instr. & Meth. B 124 (1997) 112

41. V. Koslovsky et al., Int. J. Mass Spectr. 181 (1998) 27

42. A. Dodonov et al., Eur. J. Mass Spectr. 6 (2000) 481

43. V. Raznikov et al., Rap. Comm. Mass Spectrom. 15 (2001) 1912

44. M. Gonin et al., Nucl. Instr. & Meth. B 136-138 (1998) 1244

45. R. Stresau (ETP, Sydney), priv. communication 2005

46. _____ H. Wollnik et al., Int. J. Mass Spectr. Ion Proc. 130 (1994) L7

47. B.A. Mamyrin, V.J. Karatajev, D.V.Shmikk and V.A.Zagulin, Sov. Phys. JETP 37 (1973) 45

48. H. Wollnik, patent DE3025764 of 1982

49. _____ R. Kutscher, R. Grix, G. Li and H. Wollnik, Int. J. Mass Spectr. Ion Proc. 103 (1991) 117

50. R. Cotter and W. Doroshenko, patent US 6.365,892 B1 (2002)

51. M. Yavor, A. Verenchikov, et al., Phys. Procedia 1 (2008) 391

52. H.Wollnik and M.Przewloka, Int. J. Mass Spectr. Ion Proc. 96 (1990) 267

53. _____ A. Casares, A. Kholomeev, H.Wollnik, Int. J. Mass Spectr. 227 (2003) 217

54. S. Naimi et al., Int. J. Mass Spectr. In print

55. H. Wollnik, A. Casares, D. Radford et al., Nucl. Instr. & Meth. A 519 (2004) 373

56. _____H. Balsiger et al., Adv. in Space Res. 21 (1998) 1527

57. Y. Ishida, M. Wada and H. Wollnik, Nucl. Instr. & Meth. in Phys. Res. B 241 (2005) 983

58. W.R. Plaß et al., Nucl. Instr. & Meth. in Phys. Res. B 266 (2008) 4560
59. P. Schury et al., Eur. Phys. J. A 42 (2009) 343

60. A. Piechaczek et al., Nucl. Instr. & Meth. in Phys. Res. B 266 (2008) 4510
61. R.N. Wolf et al., Nucl. Instr. & Meth. A 686 (2012) 82
62. T. Sakurai et al., Int. J. Mass Spectr. 66 (1985) 283

63. M. Ishihara et al., Int. J. Mass Spectr. 66 (1985) 283

64. T. Satoh, H. Tsuno, M. Iwagawa, Y. Kammei, J. Mass Spectr. Soc. Japan 54 (2006) 11

65. J. Tamura (JEOL, Tokyo), priv. communication 2011

66. M. Nishiguchi et al., J. Mass Spectr. Soc. Japan 44 (2009) 594

20

Graphical abstract
(a multi-pass time-of-flight mass analyzer)